

<sup>1</sup> Bhuvnesh Kumar  
Sharma<sup>2</sup> Prof. Mithilesh  
Kumar<sup>3</sup> Prof. R.S. Meena

## Exponential Characteristics of Room Impulse Response system in Noisy Environment



**Abstract:** - This paper describes the characteristics of the Room Impulse Response system for an exponential signal in presence of different noises. Traditionally Room impulse response function used for acoustic applications. Characterization of this system helps to develop its new applications. The room impulse response system is characterized using frequency domain analysis. To obtain the phase and magnitude responses, the spectrum for an exponential signal is computed and then convolved with a room impulse response system. Further the signal is exposed to the noise and then convolve it to the system and get the output for different signal to noise ratios. This whole simulation executes in MATLAB. It is discovered that the Room Impulse Response system exhibits a low pass filter magnitude response and a piecewise linear phase response when an exponential signal is applied in the presence of different noises. For varying noise levels, more parallels in the Room Impulse Response system's phase and magnitude output were discovered. This technique characterizes Room Impulse Response for exponential signals in noisy environment. A model to implement Room Impulse Response function as system also provided. Here Room Impulse Response function used as system and it is completely characterized for exponential signal in AWGN, Exponential, Rayleigh, Poisson noise. This work opens up entirely new uses for the Room Impulse Response system, like low pass and band pass filtering.

**Keywords:** Transfer function (TF), AWGN, Exponential noise, Rayleigh noise, Poisson noise, FIR filter, Room Impulse Response (RIR).

### I. INTRODUCTION

Room Impulse Responses (RIR) defined as the overall transfer function between any two places in a closed area. RIR can be divided into three parts Direct sound, Salient reflections and late reverberations for direct dependent room acoustic analysis. Traditionally this room impulse response is used for applications such as acoustic eco-cancellation, feedback cancellation and acoustic noise cancellation. A voice separation system that uses the frequency domain blind source separation technique has been developed recently with room impulse response is given in [1]. Researchers have been interested in blind source separation (BSS), which is the recovery of original source signals from observed signals without knowledge of the mixing process. Numerous applications of BSS include strong speech recognition, high-quality hearing aid equipment, crosstalk separation in telecommunication, robust speech augmentation in noisy environments, and the analysis of biological signals like magneto encephalograph (MEG) and electroencephalograph (EEG). The underlying presumption of the BSS problem is the statistical independence of the source signals.

Characterization of RIR for an exponential signal of varied width in a noise free environment given in [2]. A Spatial room impulse response calculation technique use to capture the direct sound, reflections and the reverberations. Direct and residual subspace decomposition for special room impulse response given in [3]. A technique to generate fast-diffuse RIR based on neural network for a given acoustic environment provided in [4]. Acoustic source signal travels as a spherical wave wavefront, a method using the geometric techniques to model the observed signal with image source method is provided in [5]. An estimation technique of the low rank room impulse response provided in [6]. Acoustic and audio analysis are necessary for sound field control in order to rebuild the sound field of a room. A spatio-temporal Bayesian regression for RIR reproduction with spherical waves provided in [7], where the performance given with experimental measurements and it also provides their comparison to classical Bayesian reconstruction methods. An improved room impulse response estimation technique for automatic speech recognition provided in [8]. A technique to evaluate dataset of re-transmitted speech background noise and real room impulse response given in [9]. Room impulse function depends upon many parameters such as temperature, distance between the loudspeaker and microphone, Reflection coefficient of the room, size and shape of the room.

<sup>1</sup> \*Corresponding author: Department of Electronics Engineering, Rajasthan Technical University Kota, Rajasthan, India

<sup>2</sup> Department of Electronics Engineering, Rajasthan Technical University Kota, Rajasthan, India

<sup>3</sup> Department of Electronics Engineering, Rajasthan Technical University Kota, Rajasthan, India

Correspondence: Rawatbhata road, Postal Code: 324010

E-mail: bk\_knowledge@yahoo.com, mkumar@rtu.ac.in, rsmeena@rtu.ac.in

Copyright © JES 2024 on-line : journal.esrgroups.org

Room impulse response function in different rooms provided in [10]. Blind source separation is a challenging problem in real-world environments. When there are several sources and extremely reverberant settings, this problem gets harder. One approach to source signal separation is given in [11] which, when combined with other signals, uses the higher order frequency relationships of the source signals to separate them.

In a room, the transfer function (TF) between two points represents the RIR. Rooms with different dimensions have their different RIR. The RIR is varies for different reflection coefficient of the walls of room and it also change by changing the separation between the loudspeaker and the source of the sound. In this paper, we have presented an image method which incorporates all these parameters to find the RIR. In many rooms acoustic signal processing applications, RIR identification historically required to get rid of unwanted effects like feedback, reverberation, and echo. Usually, an adaptive filter driven by an audio or voice input signal is used to do this. The recent application of room acoustic signal enhancement by incorporating the prior knowledge of the RIR for regularization is given in [12]. By using the affine projection algorithm (APA), normalized least mean square (NLMS), and recursive least square (RLS), there are numerous options for the regularization parameter have been proposed in [13], [14]–[21]. Perhaps the most well-known application, acoustic feedback suppression [22], acoustic echo cancellation with neural networks is given in [23], [24] whereby the prediction of an echo component contained in a microphone signal requires a RIR estimation.

In this paper, RIR function use as a system and its phase and magnitude characteristics are obtain using an exponential signal as the input. Further this system is test in presence of AWGN, Exponential, Rayleigh, Poisson noise. The signal to noise ratio maintains between +5dB to -4dB. An FIR structure is also proposed to implement the room impulse response system.

## II. IMAGE METHOD TO ESTIMATE ROOM IMPULSE RESPONSE

The acoustic properties between two defined places of the source and receiver are implied by the impulse response, or TF, of an enclosed room. They contain details about both reflected and direct sounds. A RIR is represented by TF between a loudspeaker and a microphone in a room when they are placed close to one another. In a room, the loudspeaker signal takes multiple routes before arriving at the microphone. A portion of the energy from the loudspeaker is directly absorbed by the microphone in the wave front of the sound energy, but the remainder of the energy travels to the microphone through numerous reflections from the room's walls. The echoes of the initial sound wave are these portions of the sound wave's energy. The echoes arrived at the microphone at varying times. These echoes leave the sound source in the form of waves, moving at a constant speed and temperature.

We present the schematic diagram to calculate the room impulse response in figure1. Where  $a_1$  and  $a_2$  represent the two virtual sources in positive and negative x direction for the two echoes and these two echoes are reaching to the microphone. We can also expand this scheme in y and z direction to obtain this scheme in three dimensions. The middle rectangle in figure1 represents the room and boundaries of that rectangle represent the walls of the room. The other rectangles represent the mirror image of the room. In those mirror images, we show the virtual sources  $a_1$  and  $a_2$  from where the microphone perceives that the sound is coming if it does not go through any reflection. Extending the vector that extends from the wall to the microphone in the room's mirror image will yield the virtual source's location. Using the calculations below, we can get the virtual source's coordinates and the virtual source's distance from the microphone.

$$x_i = (-1)^i x_a + \left[ i + \frac{1 - (-1)^i}{2} \right] x_b - x_c \quad (1)$$

$$y_j = (-1)^j y_a + \left[ j + \frac{1 - (-1)^j}{2} \right] y_b - y_c \quad (2)$$

$$z_k = (-1)^j z_a + \left[ k + \frac{1 - (-1)^k}{2} \right] z_b - z_c \tag{3}$$

$$d_{ijk} = \sqrt{x_i^2 + y_j^2 + z_k^2} \tag{4}$$

$(x_a, y_a, z_a)$  is the coordinate of the sound source,  $(x_b, y_b, z_b)$  is the room's length in x,y,z-directions. The location of the  $i^{th}$  order virtual source is calculated by adding an integer  $i$  for that virtual source. If the virtual source represents the source for single reflection rays in x direction, then  $i=1$  and if it represents the ray which undergo double reflection then  $i=2$  and so on. In the event that  $i$  is negative, the virtual source is situated on the negative x-axis; conversely, if  $i = 0$ , the virtual source is the real source. The separation between microphone and  $i^{th}$  virtual sound source is represented as  $(d_{ijk})$  and the coordinates  $(x_c, y_c, z_c)$  represent microphone's position.

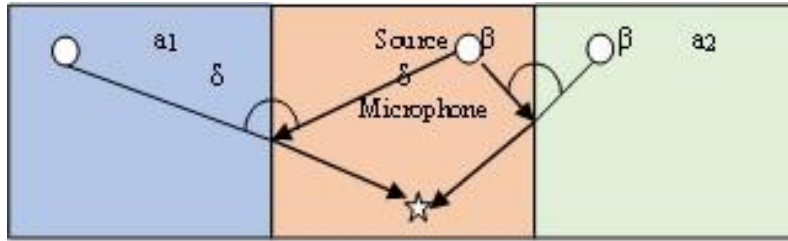


Figure1 Different echoes between microphone and loudspeaker.

After that, each echo's unit impulse response was estimated with the proper time delay to correspond to its audibility at a given location and room temperature. At last, the magnitude of each echo calculated for the unit impulse response. The amplitude of each impulse is attenuated because of the total distance travel by the impulse from microphone to source and due to reflection coefficient of wall. The amplitude of each echo attenuates with the inverse of the distance travelled by that echo before reaching to microphone. If the wall's reflection coefficient in x direction is represented by  $r_i$  then the total attenuation will be  $e_i = r_i / d_i$ . The magnitude of the impulse can be estimated for three dimensions case as:

$$e_{ijk} = b_{ijk} r_{ijk} \tag{5}$$

$$b_{ijk} \propto \frac{1}{d_{ijk}} \tag{6}$$

$$r_{ijk} = r_w^{|i|+|j|+|k|} \tag{7}$$

where  $r_w$  is the wall reflection coefficient.

In this way, the magnitude and time of each echo estimated as it is listened from a particular location in a room. If we calculate each echo at  $t = d_i / c_i$  then that echo can be represented by an impulse. Where  $c$  represents the velocity of sound at a particular temperature and  $i$  represents the index for  $i^{th}$  virtual source in x direction. By taking the summation in all three directions, we can get the total impulse response of the room. We put all the above information together with an one-dimensional time function then this will be RIR.

$$h(t) = \sum_{i=-l}^l \sum_{j=-l}^l \sum_{k=-l}^l e_{ijk} a\left(t - \frac{d_{ijk}}{c_{air}}\right) \tag{8}$$

Where  $a\left(t - \frac{d_{ijk}}{c_{air}}\right)$  is one only at  $t - \frac{d_{ijk}}{c_{air}}$

$$c_{air} = 331.3 \sqrt{1 + \frac{T}{273.15}} ms^{-1} \tag{9}$$

The temperature is represented by  $T$  in ( $^{\circ}C$ ). In equation (8) impulse response made discrete by sampling. The discrete time will allow us to use it as finite impulse response filter (FIR) for simulating it [25]. Finally, we have RIR in discrete time as:

$$h(n) = \sum_{i=-l}^l \sum_{j=-l}^l \sum_{k=-l}^l e_{ijk} a\left(\frac{n}{f_s} - \frac{d_{ijk}}{c_{air}}\right) \tag{10}$$

Where  $l=|i|+|j|+|k|$  represents sound wave's total number of reflections,  $e_{ijk}$  represents the each echo magnitude, which depends upon attenuation got by the each echo while completing the different distances and with consideration of reflection coefficient of the walls,  $n$  represent the sampling time,  $f_s$  represents the frequency of sampling,  $d_{ijk}$  stands for distance travelled by each echo,  $c_{air}$  is the sound velocity,  $i$  represents index for  $i^{th}$  virtual source at positive x,  $j$  represents the index for  $j^{th}$  virtual source at positive y,  $k$  represents the index for  $k^{th}$  virtual source at positive z. Figure2 is a simplified illustration for the typical form of RIR. In Figure 2 the lower order, early reflection and the direct sound impulses are clearly shown. After that the impulses of RIR are denser so that the discrimination between the individual impulses cannot be made easily. Denser part of RIR known as reverberation tail. The sound intensity will drop with the square inverse of distance travelled  $1/r^2$  by the sound wave. Here we have to consider a point significantly that the measurement of RIR by real instruments always done with a running time window due to the low pass characteristics of it. So all RIR curves shows same envelopes up to no absorption or dissipation occurred. Consequently in the running time window the energy overtime is constant.

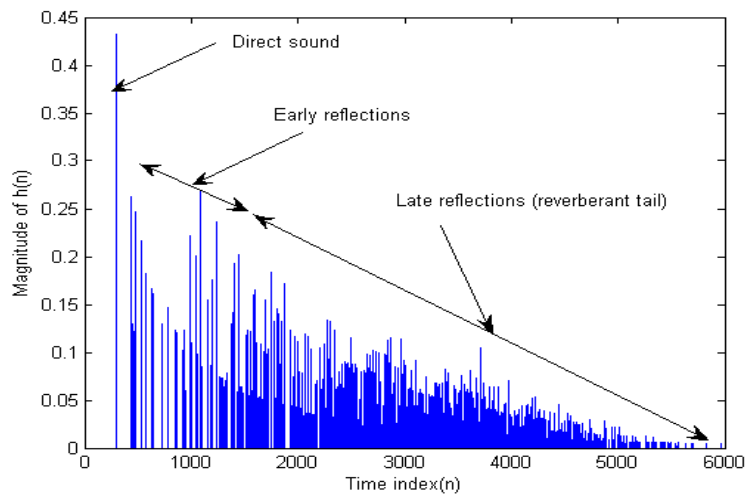


Figure 2 Room impulse response

### III. SYSTEM MODEL

In this section, we have proposed a direct form structure to implement RIR as shown by the equation (10) and this structure could be integrated in the form of the filtering core [18]. We have used the direct structure to represent the

filter because the direct structures are very easy to implement and have lower complexity. If we have  $M$  distinct values for  $P$  then this structure requires  $M^M$  number of memory elements,  $M^M - M$  additions and  $M^M$  multiplications are required per output point. The input  $a(n)$  is the sequence in which all samples are having value equal to zero except the sample number as  $\frac{d_{ijk} * f_s}{c_{air}}$ . On these sample numbers, the value of  $a(n)$  is equal to one and  $a(n)$  is applied to the input of the filter with the sampling frequency  $f_s$ .

We can write equation (10) as:

$$\begin{aligned}
 h(n) = & \sum_{i=-1}^1 e_{i-1-1} a\left(\frac{n}{f_s} - \frac{d_{i-1-1}}{c_{air}}\right) + \sum_{i=-1}^1 e_{i-0-1} a\left(\frac{n}{f_s} - \frac{d_{i-0-1}}{c_{air}}\right) + \sum_{i=-1}^1 e_{i1-1} a\left(\frac{n}{f_s} - \frac{d_{i1-1}}{c_{air}}\right) + \sum_{i=-1}^1 e_{i-10} a\left(\frac{n}{f_s} - \frac{d_{i-10}}{c_{air}}\right) \\
 & + \sum_{i=-1}^1 e_{i100} a\left(\frac{n}{f_s} - \frac{d_{i100}}{c_{air}}\right) + \sum_{i=-1}^1 e_{i10} a\left(\frac{n}{f_s} - \frac{d_{i10}}{c_{air}}\right) + \sum_{i=-1}^1 e_{i-11} a\left(\frac{n}{f_s} - \frac{d_{i-11}}{c_{air}}\right) + \sum_{i=-1}^1 e_{i01} a\left(\frac{n}{f_s} - \frac{d_{i01}}{c_{air}}\right) \\
 & + \sum_{i=-1}^1 e_{i11} a\left(\frac{n}{f_s} - \frac{d_{i11}}{c_{air}}\right)
 \end{aligned}
 \tag{11}$$

In figure3, we have presented a scheme to construct the architecture given in equation (11) for  $f_s = 1$  Hz. To construct the architecture, we have used the direct form structure which is given in [25], [26]. Each block can be made by the structure shown in figure 4 for all values of  $i$  and one combination of  $j, k$  for that block. The next block of figure3 can be made by taking the next combination of  $j, k$  for figure4 and so on. In this way, we can construct the whole architecture of RIR.

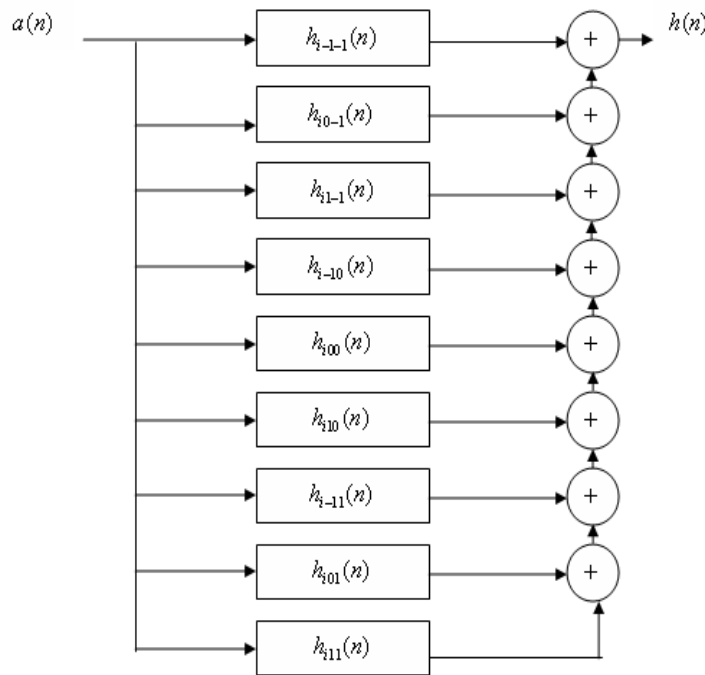


Figure 3 The proposed FIR structure for room impulse response for  $i = -1, 0, 1$ .

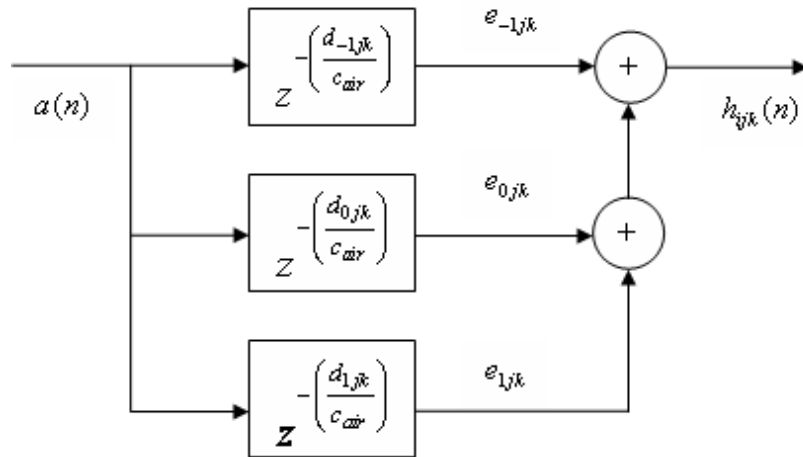


Figure 4 Proposed structure for one block shown in previous figure3 for all  $j, k$  combinations.

**IV. MATHEMATICAL MODEL**

As we discuss previously, we can model our RIR according to the equation (10). For a large number of reflections of sound wave through the walls of the room the RIR coefficients generated are also very large. In this situation it is very difficult to study the RIR because the mathematical expression at that time is very complex and the visualization between different output characteristics of the RIR is very complex and the observations are very difficult. To reduce the complexity of the system and to determine the nature of the different sets of the output and to get the conclusion, RIR with few coefficients as parameters given in table 1 is calculated. Here  $l=1$  took, while  $i = 1, j = k = 0$ . This RIR is plotted in figure 5.

Table 1: Different Parameter for determination of RIR

Loudspeaker' location in meters	4,4,4
Microphone's location in meters	3,3,3
Room Length, High, Width in meters	5,5,5
Temperature of room in $^{\circ}\text{C}$	27
Virtual source order	1
Sampling frequency in Hz	440
Room wall Reflection coefficient	0.3

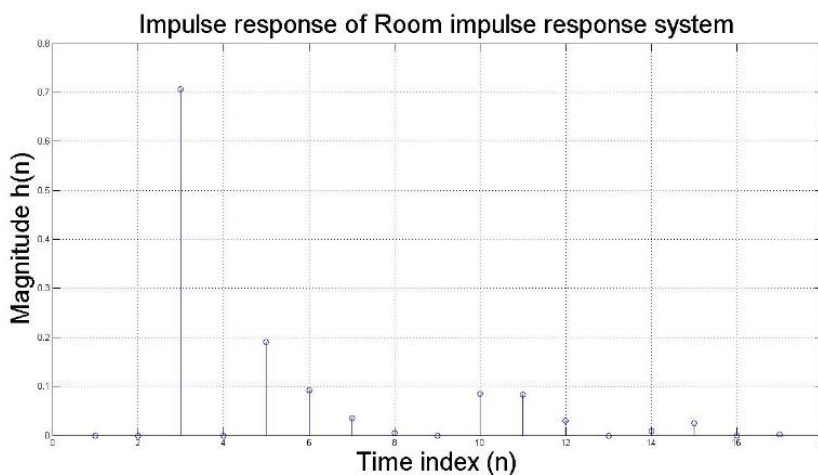


Figure 5 Room impulse response

We can expand the equation (10) by taking the values of  $i=1, j=k=0$  as mentioned above. Now to calculate RIR, we first obtain the values of  $n$  for which the impulses are present for the different values of  $i, j, k$ . The different values of  $n$  for the values given in Table1 are as:

$$\begin{aligned}
 n(:, :, 1) &= \begin{pmatrix} 17 & 15 & 15 \\ 15 & 11 & 12 \\ 15 & 12 & 12 \end{pmatrix} \\
 n(:, :, 2) &= \begin{pmatrix} 14 & 10 & 11 \\ 10 & 3 & 5 \\ 11 & 5 & 6 \end{pmatrix} \\
 n(:, :, 3) &= \begin{pmatrix} 15 & 11 & 12 \\ 11 & 6 & 7 \\ 12 & 7 & 8 \end{pmatrix}
 \end{aligned} \tag{12}$$

These index values of  $n$  give the values for corresponding  $(i, j, k)$ . For these  $i, j, k$  we calculate the different values of  $(e_{ijk})$  which are given as:

$$\begin{aligned}
 e(:, :, 1) &= \begin{pmatrix} 0.0021 & 0.0084 & 0.0024 \\ 0.0084 & 0.0369 & 0.0105 \\ 0.0024 & 0.0105 & 0.0030 \end{pmatrix} \\
 e(:, :, 2) &= \begin{pmatrix} 0.0091 & 0.0424 & 0.0118 \\ 0.0424 & 0.7071 & 0.0949 \\ 0.0118 & 0.0949 & 0.0212 \end{pmatrix} \\
 e(:, :, 3) &= \begin{pmatrix} 0.0025 & 0.0111 & 0.0031 \\ 0.0111 & 0.0707 & 0.0177 \\ 0.0031 & 0.0177 & 0.0046 \end{pmatrix}
 \end{aligned} \tag{13}$$

If we add all the values of error indexed by the particular value of  $n$  then we get the RIR for that particular value of  $n$ . For example, to obtain the value of RIR at  $n=11$ . We have to add up the values 0.0369, 0.0118, 0.0118, 0.0111 and 0.0111 respectively and finally obtained 0.0827, which is the value of RIR at  $n=6$ . According to this, the RIR become as:

$$\begin{aligned}
 h(n) &= [0 \quad 0 \quad 0.7071 \quad 0 \quad 0.1897 \quad 0.0919 \quad 0.0353 \quad 0.0046 \quad 0 \quad 0.0849 \quad 0.0827 \quad 0.0302 \\
 &\quad 0 \quad 0.0091 \quad 0.0243 \quad 0 \quad 0.0021]
 \end{aligned} \tag{14}$$

We have plotted the phase and magnitude spectrum of  $h(n)$  in figure6 and figure7 respectively.

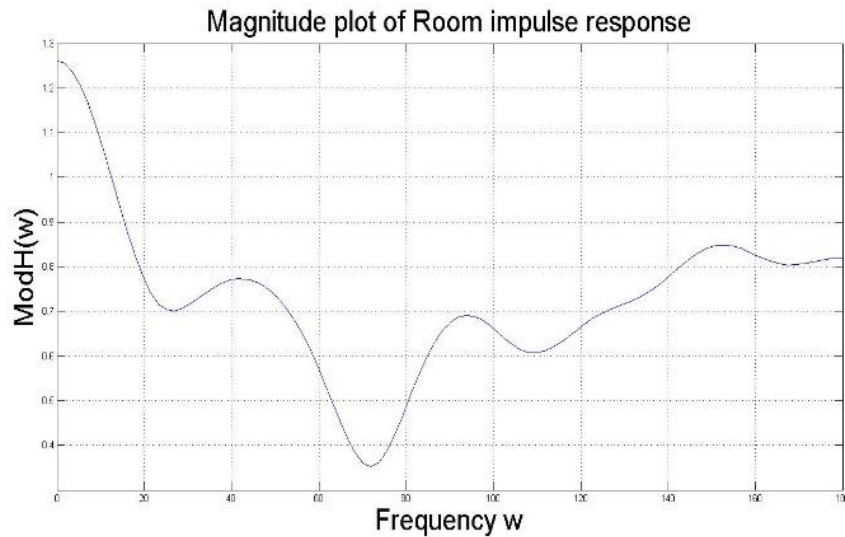


Figure 6 Magnitude plot of  $h(n)$

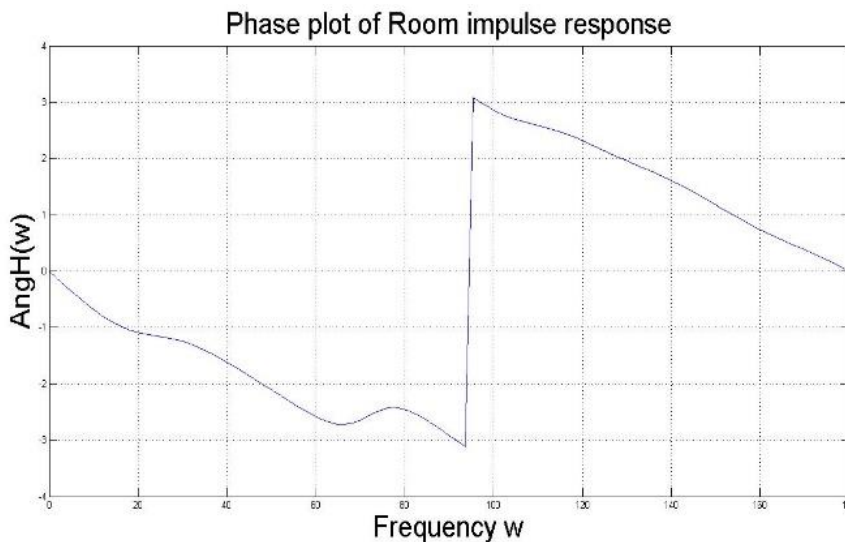


Figure 7 Phase plot of  $h(n)$

**V. EXPONENTIAL SIGNAL**

Exponential signals are widely used to study the basic behaviour of the system in signal processing and control systems and to study the RC characteristics of a network. Exponential signals are widely used in engineering, economics and physics. Exponential signals are defined as Real exponential signal and Complex exponential signal and its mathematical equation given as below:

$$x(t) = Ae^{(\alpha + j\beta)t} \tag{15}$$

$A$  represents amplitude.

$e$  represents base of the natural logarithm.

$\alpha$  and  $\beta$  represents real numbers.

$j$  represents imaginary unit

$t$  represents time.

**VI. PHASE AND MAGNITUDE RESPONSE  $H(N)$  FOR EXPONENTIAL SIGNAL**

To calculate the response of a RIR for exponential signals, The exponential input defined as:

$$\exp(n) = \sum_{k=0}^{31} \exp \delta(n-k) \tag{16}$$

The total input sequence length is thirty-two samples taken for calculation. The output  $\exp_{ai}(n)$  for RIR  $h(n)$  for the given exponential inputs given as:

$$h(n) = x_r(n) + jx_i(n) \tag{17}$$

$$\exp_{ai}(n) = \exp(n) * (x_r(n) + jx_i(n)) \tag{18}$$

$$\exp_{ai}(n) = \exp(n) * (x_r(n)) + \exp(n) * (jx_i(n)) \tag{19}$$

$$|Mag(n)| = \sqrt{\left(\sum_{k=0}^{31} \exp(k)x_r(n-k)\right)^2 + \left(\sum_{k=0}^{31} \exp(k)x_i(n-k)\right)^2} \tag{20}$$

$$Ang(n) = \tan^{-1} \left( \frac{\left(\sum_{k=0}^{31} \exp(k)x_i(n-k)\right)}{\left(\sum_{k=0}^{31} \exp(k)x_r(n-k)\right)} \right) \tag{21}$$

**VII. RIR SYSTEM CHARACTERISTICS IN NOISY ENVIRONMENT**

Here the output of RIR system is analysed for input exponential signal in presence of four different commonly used noises. To study a communication system, to find out the response of the system, to make adjustments in our transmitted signal there are generally four types of noises are studies. These are AWGN noise, Rayleigh noise, Poisson noise and Exponential noise. Figure8 shows the block diagram used to characterize the RIR system.

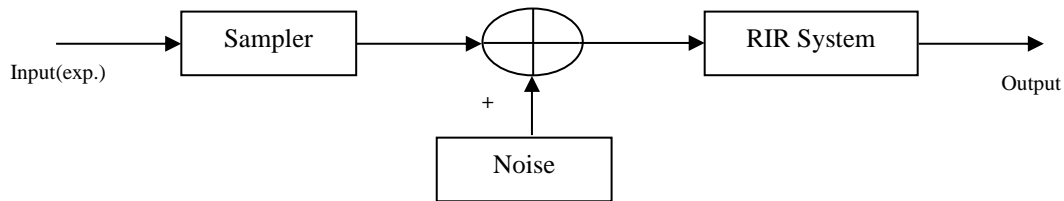


Figure 8 Scheme for analysis of RIR system in noisy environment

**VIII. AWGN NOISE**

Additive White Gaussian (AWGN) generally produced in a communication system due to the random disturbances. AWGN is generally used to model the overall noise characteristics of a communication system. AWGN has flat frequency spectrum so its power equally distributed in complete spectrum of the noise. The noise power can be calculated by its variance for a system. AWGN noise used to model the real-world noise mathematically. To study a system AWGN noise generally used to characterise that system or to find the system behaviour in presence of noise.

In this paper AWGN is used with zero mean and its power spectral density given as:

$$f_{aw}(n) = \frac{1}{\sqrt{2\pi\sigma_{aw}}} \exp \left[ -\frac{(n - \mu_{aw})^2}{2\sigma_{aw}^2} \right] \tag{22}$$

$$\mu_{aw} = \text{mean}$$

$$\sigma_{aw} = \text{variance}$$

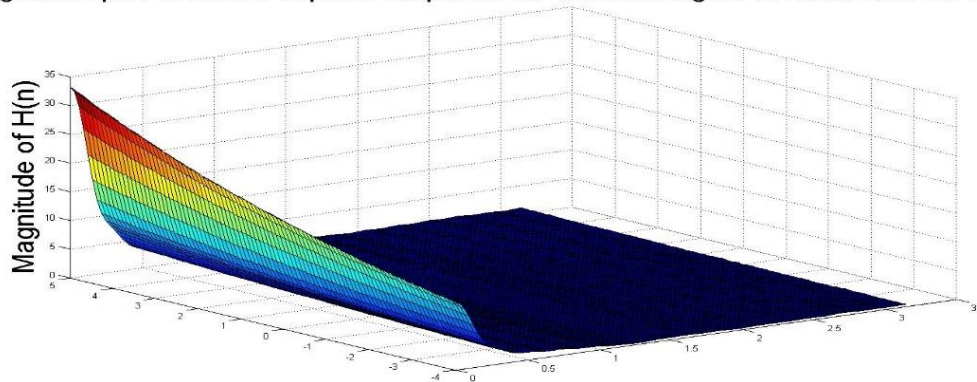
Here we take mean = 0

$$\text{Signal to noise ratio} = \left[ 10 \log_{10} \frac{A^2}{\sigma_{aw}^2} \right] \tag{23}$$

A = Amplitude of the signal

It is clearly observed from the figure 6 that the energy in the main lobe of the output is decreases on decreasing signal to noise ratio (SNR) from +5 dB to -4dB.

Magnitude plot of Room impulse response for different signal to noise ratio for AWGN

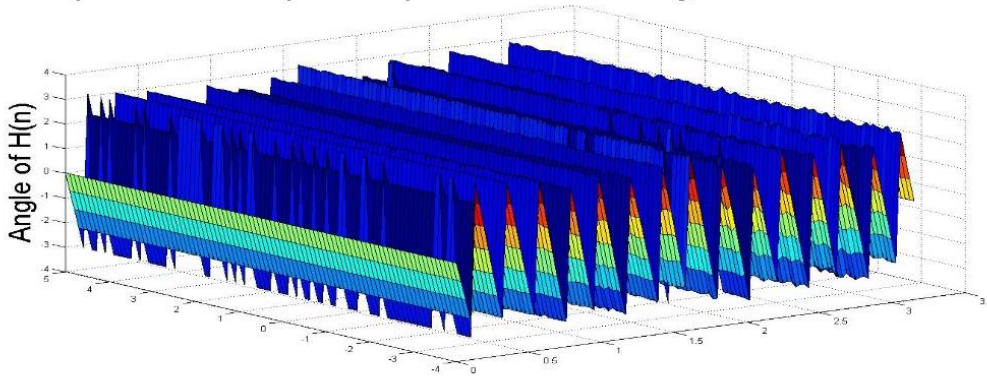


Signal to noise ratio dB

Frequency(w)

Figure 9 Magnitude plot of RIR system for different signal to noise ratio for AWGN

Phase plot of Room impulse response for different signal to noise ratio for AWGN



Signal to noise ratio dB

Frequency(w)

Figure10 Phase plot of RIR system for different signal to noise ratio for AWGN

### IX. RAYLEIGH NOISE IN COMMUNICATION SYSTEMS

When signal propagates through a wireless medium then a random variation in amplitude due to the scattering is generally called Rayleigh noise. From the transmitter to the receiver Rayleigh noise is basically the scattering effect on the electromagnetic waves by the small objects in the propagation medium. When the wave travelling from transmitter to the receiver in the propagation medium, between the path wave scatters and it reaches to the receiver by following the multiple paths and it make the fading at the receiver. A special case of two wave with diffuse power feeding is called Rayleigh fading in wireless communication systems. The Rayleigh fading has significant effect and in many cases it drops the signal power to zero, which creates error in data transmission. The power spectral density function for Rayleigh distribution is given as:

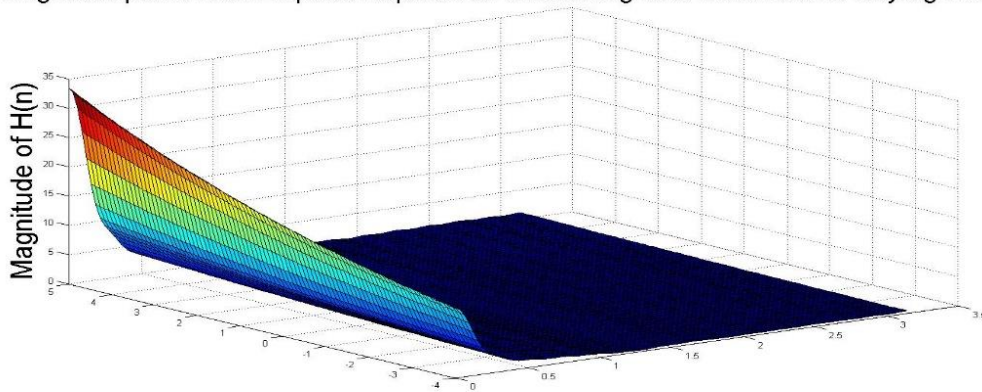
$$f_{ray}(n) = \frac{x}{c^2} e\left(-\frac{x^2}{2c^2}\right) \tag{24}$$

c = parameter

$$\text{Signal to noise ratio} = \left[ 10\log_{10} \frac{A^2}{c^2} \right] \tag{25}$$

A = Amplitude of the signal

Magnitude plot of Room impulse response for different signal to noise ratio for Rayleigh Noise

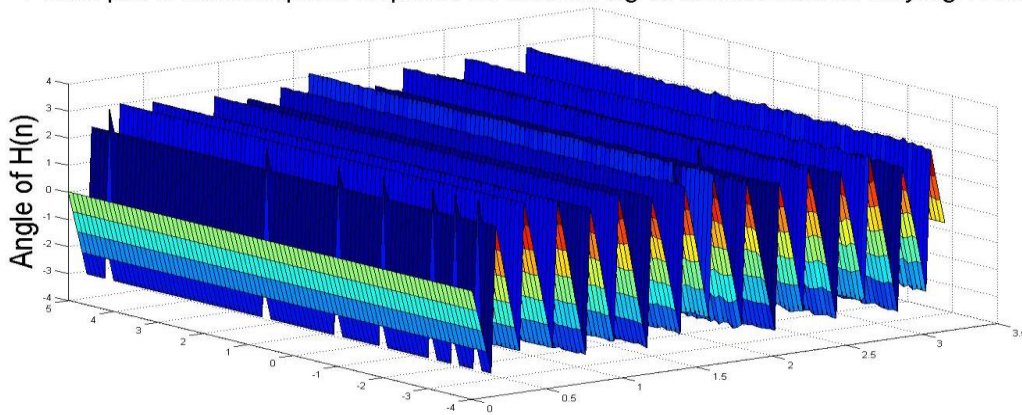


Signal to noise ratio dB

Frequency(w)

Figure11 Magnitude plot of RIR system for different signal to noise ratio for Rayleigh noise.

Phase plot of Room impulse response for different signal to noise ratio for Rayleigh Noise



Signal to noise ratio dB

Frequency(w)

Figure 12 Phase plot of RIR system for different signal to noise ratio for Rayleigh noise.

### X. POISSON NOISE

Poisson noise commonly analyse in an optical communication system. In an optical communication system when the signal is generated in the form of light the noise is occurred due to the random behaviour transmitted photons travelling in the optical medium and arrive at the receiver in a random manner.

The power spectral density function for Poisson distribution is:

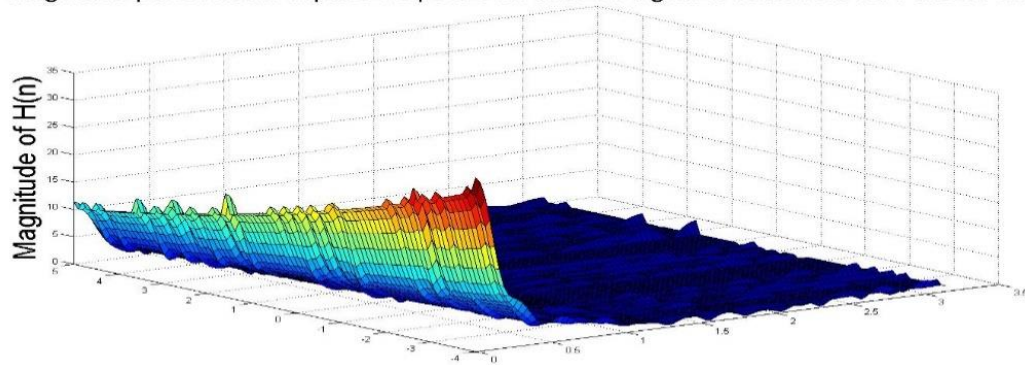
$$f_{poi}(n) = \frac{\mu^n}{x} e^{-\mu} \tag{26}$$

$\mu = \text{mean}$

$$\text{Signal to noise ratio} = \left[ 10 \log_{10} \frac{A^2}{\mu} \right] \tag{27}$$

A= Amplitude of the signal

Magnitude plot of Room impulse response for different signal to noise ratio for Poisson Noise

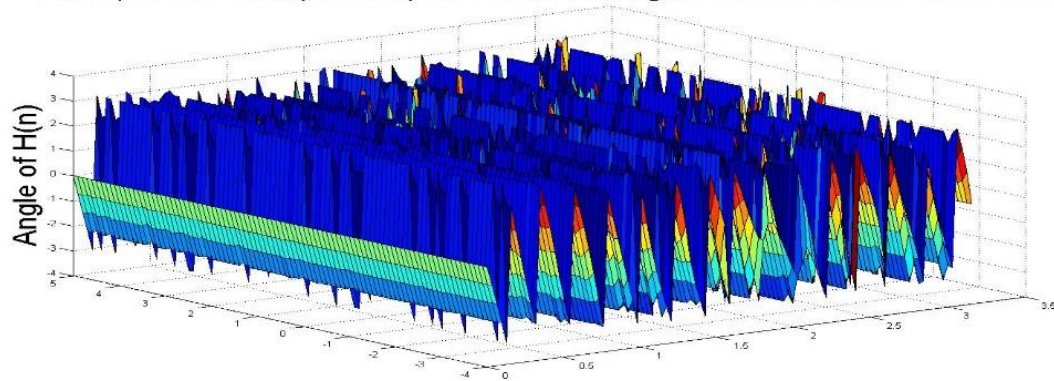


Signal to noise ratio dB

Frequency(w)

Figure 13 Magnitude plot of RIR system for different signal to noise ratio for Poisson noise.

Phase plot of Room impulse response for different signal to noise ratio for Poisson Noise



Signal to noise ratio dB

Frequency(w)

Figure 14 Phase plot of RIR system for different signal to noise ratio for Poisson noise.

### XI. EXPONENTIAL NOISE

The source of Exponential noise in a communication system are interference, shot noise, thermal noise and other random processes by which random variations in the signal amplitude occurred. The power spectral density function for exponential distribution is:

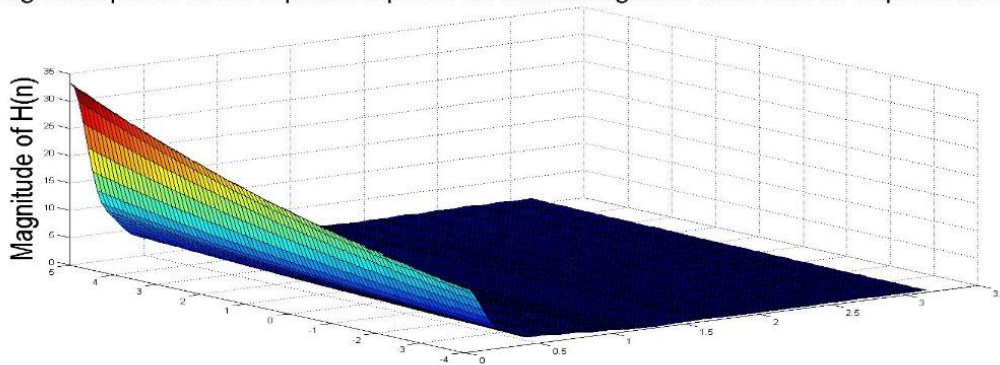
$$f_{\text{exp}}(n) = \frac{1}{\mu} e^{-\frac{n}{\mu}} \tag{28}$$

$\mu = \text{mean}$

$$\text{Signal to noise ratio} = \left[ 10 \log_{10} \frac{A^2}{\mu} \right] \tag{29}$$

A= Amplitude of the signal

Magnitude plot of Room impulse response for different signal to noise ratio for Exponential Noise

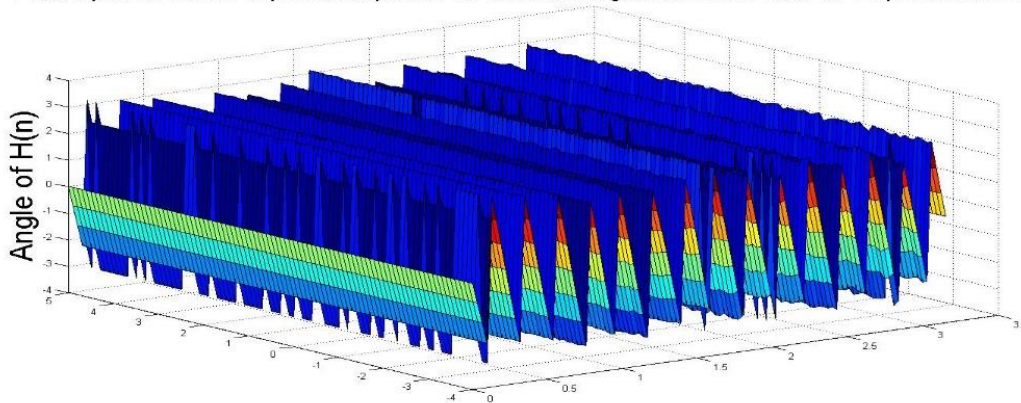


Signal to noise ratio dB

Frequency(w)

Figure 15 Magnitude plot RIR system for different signal to noise ratio for Exponential noise.

Phase plot of Room impulse response for different signal to noise ratio for Exponential Noise



Signal to noise ratio dB

Frequency(w)

Figure 16 Magnitude plot of RIR system for different signal to noise ratio for Exponential noise.

## XII. CONCLUSION

Here RIR system is successfully characterize in terms of magnitude and phase spectrum for exponential signal in presence of different noise. Figure 9 & 10 shows the output of RIR system for AWGN noise. It is clearly observed from figure 9 that the shape of magnitude remains low pass filter for signal to noise ratio +5dB to -4dB, but peak value of the output curve is decrease on decreasing the signal to noise ratio. Energy in main lobe of magnitude plot is also decrease with the signal to noise ratio. Figure 10 shows that the phase characteristics of RIR system are minimum phase which required for a stable system. Phase characteristics are piecewise linear also and they have no significant change with noise. This same phase and magnitude response of RIR for the Rayleigh noise shown in figures 11&12, for the Poisson noise shown in figures 13&14, for the Exponential noise shown in figures 15&16. In future by using this characterization, RIR system can be used for low pass, band pass filtering and for frequency separation in noisy environment.

## ADDITIONAL INFORMATION

**Funding:** None

**Conflicts of interest:** no conflicts related to this work

**Consent for publication:** Informed consent was obtained from all the Authors.

## REFERENCES

- [1] Bhuvnesh Kumar Sharma, Mithilesh Kumar, R. S. Meena, "Development of a speech separation system using frequency domain blind source separation technique," *Multimedia Tools and Applications*, 2023, vol.83, pp.32857–32872, <https://doi.org/10.1007/s11042-023-16600-6>.
- [2] B. K. Sharma, Mithilesh Kumar, R. S. Meena, "Phase and Amplitude Characterization of Room Impulse Response on the Application of Varied Width Exponential Signals," *Power Engineering and Intelligent Systems Proceedings of PEIS 2023*, 2023, vol.2, pp.425-434, [https://link.springer.com/chapter/10.1007/978-981-99-7383-5\\_32](https://link.springer.com/chapter/10.1007/978-981-99-7383-5_32).
- [3] Thomas Deppisch, Sebastià V. Amengual Garí and Jens Ahrens, "Direct and Residual Subspace Decomposition of Spatial Room Impulse Responses," *IEEE/ACM transactions on audio, speech, and language processing*, 2023, vol.31, pp.927-948, <https://ieeexplore.ieee.org/document/10028731>.
- [4] Anton Ratnarajah, Shi-Xiong Zhang, Meng Yu, Zhenyu Tang, Dinesh Manocha, Dong Yu, "Fast-RIR fast neural diffuse room impulse response generator," *ICASSP-2022 IEEE International Conference on Acoustics, Speech and Signal Processing*. 2022, <https://ieeexplore.ieee.org/document/9747846>.
- [5] Jiarui Wang, Prasanga Samarasinghe, Thushara Abhayapala, "Jihui Aimee Zhang, Image source method based on the directional impulse responses," *ICASSP 2023 IEEE International Conference on Acoustics, Speech and Signal Processing (ICASSP)*, 2023, <https://ieeexplore.ieee.org/document/10095916>.
- [6] Martin Jälmbly, Filip Elvander, Toon van Waterschoot. Low-Rank Room Impulse Response Estimation, "IEEE/ACM Transactions on audio, speech, and language processing," 2023, vol.31, pp.957-969. <https://ieeexplore.ieee.org/document/10028766>.
- [7] Diego Caviedes-Nozal, EfenFernandez-Grande. Spatio-Temporal Bayesian Regression for Room Impulse Response Reconstruction With Spherical Waves. *IEEE/ACM Transactions on audio, speech, and language processing*. 2023; 31: 3263-3277. <https://ieeexplore.ieee.org/document/10226555>.
- [8] Anton Ratnarajah, Ishwarya Ananthabhotla, Vamsi Krishna Ithapu, Pablo Hoffmann, Dinesh Manocha, Paul Calamia, "Towards improved room impulse response estimation for speech recognition," *ICASSP-2023 IEEE International Conference on Acoustics, Speech and Signal Processing (ICASSP)*, 2023, <https://ieeexplore.ieee.org/document/10094770>.
- [9] Igor Szöke, Miroslav Skácel, Ladislav Mošner, Jan (Honza)Cernocký, "Building and Evaluation of a Real Room Impulse Response Dataset," *IEEE Journal of selected topics in signal processing*, 2019, vol.13, pp. 863-876, <https://ieeexplore.ieee.org/document/8717722>.
- [10] J. Mourjopoulos, "On the variation and invertibility of room impulse response functions," *Journal of Sound and Vibration*, 1985, vol.102(2), pp.217-228, <https://www.sciencedirect.com/science/article/abs/pii/S0022460X85800547>.
- [11] Taesu Kim ,T. Attias, Soo-Young Lee, Te-Won Lee, "Blind Source Separation Exploiting Higher-Order Frequency Dependencies," *IEEE Transection on Speech and language processing*, 2007, vol.15, pp.70-79, <https://ieeexplore.ieee.org/document/4032777>.
- [12] Toon van Waterschoot, Geert Rombouts, Marc Moonen, "Optimally regularized adaptive filtering algorithms for room acoustic signal enhancement," *Elsevier Signal Processing*, 2008, vol.88, pp. 594–611. <https://www.sciencedirect.com/science/article/abs/pii/S0165168407003179>.
- [13] G.Rombouts, T. van Waterschoot, K. Struyve, M. Moonen, "Acoustic feedback suppression for long acoustic paths using a nonstationary source model," *IEEE Transection on Signal Process*, 2006, vol. 54 (9), pp. 3426–3434. <https://ieeexplore.ieee.org/document/1677908>.
- [14] Z. Chen, S. Haykin, S.L. Gay, "Proportionate adaptation: new paradigms in adaptive filtering," S. Haykin, B.Widrow (Eds.), *Advances in LMS filters*, New York, Wiley,2003 (Chapter 8).
- [15] T. Gansler, J. Benesty, S.L. Gay, M.M. Sondhi, "A robust proportionate affine projection algorithm for network echo cancellation," in: *Proceedings of the 2000 IEEE International Conference on Acoustics, Speech, and Signal Processing (ICASSP 2000)*, 2000, <https://ieeexplore.ieee.org/document/859079>.
- [16] T.Y. Al-Naffouri, A.H. Sayed, "An adaptive filter robust to data uncertainties," in: *Proceedings of the Allerton Conference on Communication, Control and Computing*, 2000, [https://www.researchgate.net/publication/2315112\\_An\\_Adaptive\\_Filter\\_Robust\\_to\\_Data\\_Uncertainties](https://www.researchgate.net/publication/2315112_An_Adaptive_Filter_Robust_to_Data_Uncertainties).
- [17] T. Gansler, S.L. Gay, M.M. Sondhi, J. Benesty, "Double-talk robust fast converging algorithms for network echo cancellation," in: *Proceedings of the 1999 IEEE Workshop on Applications on Signal Processing to Audio and Acoustics (WASPAA 99)*, 1999, <https://ieeexplore.ieee.org/document/810888>.

- [18] B. Baykal, A.G. Constantinides, "Underdetermined-order recursive least-squares adaptive filtering: the concept and algorithms," *IEEE Transaction on Signal Process*, 1997, vol.45 (2), pp.346–362, <https://ieeexplore.ieee.org/document/554300>.
- [19] M. Bodson, "An adaptive algorithm with information dependent data forgetting," in: *Proceedings of the 1995 American Control Conference (ACC '95)*, 1995, <https://ieeexplore.ieee.org/document/533784>.
- [20] S.L. Gay, "Dynamically regularized fast RLS with application to echo cancellation," in: *Proceedings of the 1996 IEEE International Conference on Acoustics, Speech, and Signal Processing (ICASSP '96)*, 1996. <https://ieeexplore.ieee.org/document/543281>.
- [21] D.R. Morgan, S.G. Kratzer, "On a class of computationally efficient, rapidly converging, generalized NLMS algorithms. *IEEE Signal Processing letters*," 1996, vol.3 (8), pp.245–247, <https://ieeexplore.ieee.org/document/511808>.
- [22] G.Rombouts, T. van Waterschoot, K. Struyve, M. Moonen, "Acoustic feedback suppression for long acoustic paths using a non stationary source model," *IEEE Transaction on Signal Processing*, 2006, vol.54 (9), pp. 3426–3434. <https://ieeexplore.ieee.org/document/1677908>.
- [23] A. Ben Rabaa, Rached Tqurki, "Acoustic Echo Cancellation based on a Recurrent Neural Network and a Fast Affine Projection," *IECON '98 Proceedings of the 24th Annual Conference of the IEEE Industrial Electronics Society (Cat. No.98CH36200)*, 1998, <https://ieeexplore.ieee.org/abstract/document/722948>.
- [24] A. N. Birkett, R. A. Goubran, "Acoustic echo cancellation using NLMS-NEURAL NETWORK structure. 1995 International Conference on Acoustics, Speech, and Signal Processing," 1995, <https://ieeexplore.ieee.org/document/479485>.
- [25] John G. Proakis, Dirmirtis G. Manolakis, "Digital signal processing Principals Algorithms and Applications," Third edition, Pearson Education, 2004, pp.503-510.